Analyzing Deformation of a Cationic Polymerization UV Curable Adhesive during the Curing Process in Bonding of Optical Components

Akari Takahashi[1]

In the manufacturing of optical products, precision bonding technology, which mounts optical components with high positional accuracy, is an important fundamental technology. To achieve high positional accuracy, it is essential to comprehend the deformation of the adhesive joint over time during processing. Therefore, a method to analyze the displacement of optical components resulting from the deformation of a cationic polymerization UV curable adhesive was developed. First, the physical properties of the adhesive were formulated. Then equations, governing the adhesive properties, were used to perform finite element method (FEM) simulations to analyze the position of the optical component during curing of the adhesive. Experimental tests on adhesively bonded components were also conducted under conditions identical to those employed in the simulation. The results of the simulation and experiment exhibited a consistent trend, indicating the effectiveness of the modeling and simulation methods employed in this study.

1. Introduction

In the housings of optical products, optical systems consisting of optical components such as lenses and mirrors are constructed. Optical components are adjusted along the optical axis and fixed at the appropriate position and angle. In order to achieve this process, it is desirable to use a fixing method that can be joined in a timely manner and within a short period. In addition, it is necessary to bond dissimilar materials such as optical components (glass) and housings (metal). For this reason, UV curable adhesives are commonly used to mount optical components.

One issue in the manufacturing of optical products is displacement of the components from their original positions caused by the expansion and shrinkage of the adhesive layers. Mounting optical components requires extremely high positional accuracy, and even sub-micrometer misalignment would lead to degradation of their optical characteristics. Precise adhesion is indispensable for the development of optical products. One essential factor in achieving precise adhesion is understanding the curing process of adhesives. The curing process involves not only simple shrinkage due to the curing reaction, but also significant change in mechanical properties, namely a transition from viscosity to viscoelasticity. This process would affect the long-term reliability of products because of the relaxation of internal stresses caused by curing.

Commonly, optimizing adhesive structures and processes required experimental approaches involving numerous prototypes, which took a great deal of time in development. Quantitative prediction of the deformation of adhesive parts under arbitrary curing conditions would realize optical products with higher performance and better reliability in shorter time. Therefore, I developed a method to analyze the displacement of optical components resulting from the deformation of adhesive during the curing process of a cationic polymerization UV curable adhesive as an example.

2. Modeling of adhesive joints

2.1 Adhesive structure

This study employed an epoxy resin-based cationic polymerization UV curable adhesive that contained an iodonium salt-type initiator. A silica filler was also filled in the adhesive to minimize expansion and shrinkage of the volume. This type of adhesive is often used for the fabrication of optical products due to the small curing shrinkage, no oxygen inhibition, and superior heat resistance. On the other hand, in photocationic polymerization, it is known that the curing reaction continues as a dark reaction even after the UV irradiation 1) 2), and this characteristic makes it difficult to control the curing reaction.

Figure 1 shows the adhesive structure discussed in this study. A glass component was bonded to a copper substrate using the adhesive. The adhesive part includes an adhesive layer at the bottom of the glass component and fillets formed on the edges of the glass component. The fillets formed as shown in Fig. 1 when the glass component was placed on the adhesive that was applied in a certain amount because this adhesive has high viscosity. The dimensions in Fig. 1 were measured using the sample after the curing process. A UV light source for curing the adhesive was placed diagonally above the glass component, and UV

---

[1] : Optical Technologies R&D Center

Abbreviations, Acronyms, and Terms.

Cationic polymerization—
A polymerization reaction in which positively charged ions (cations) serve as chain-initiating species.

FEM—Finite Element Method
A numerical analysis method that divides complex structures or physical phenomena into small elements and solves approximate equations for each element to determine the overall behavior.

Storage modulus —
Real part of the complex elastic modulus. Also called the dynamic elastic modulus. It is a physical quantity indicating a material's ability to elastically store deformation energy from external forces, serving as an indicator of stiffness or hardness.

Loss modulus —
Imaginary part of the complex elastic modulus. It is a physical quantity indicating a material's ability to dissipate deformation energy from external forces in the form of heat or other energy, serving as an indicator of viscosity.

Master curve—
A curve representing the material's behavior over a wide range of time or frequency by superimposing viscoelastic properties at different temperatures along the time or frequency scale.

Rheometer—
A device for evaluating the properties of materials such as viscosity, deformation, and flow.

DMA—Dynamic Mechanical Analysis
A method for measuring mechanical properties by applying vibrational strain or stress to a material and measuring the resulting stress or strain response.

Laser displacement meter—
A device that non-contact measures the position, distance, and displacement of an object by irradiating it with laser beam.

Coherence scanning interferometer—
A device that measures the surface shape of an object precisely and non-contact using white light interference.

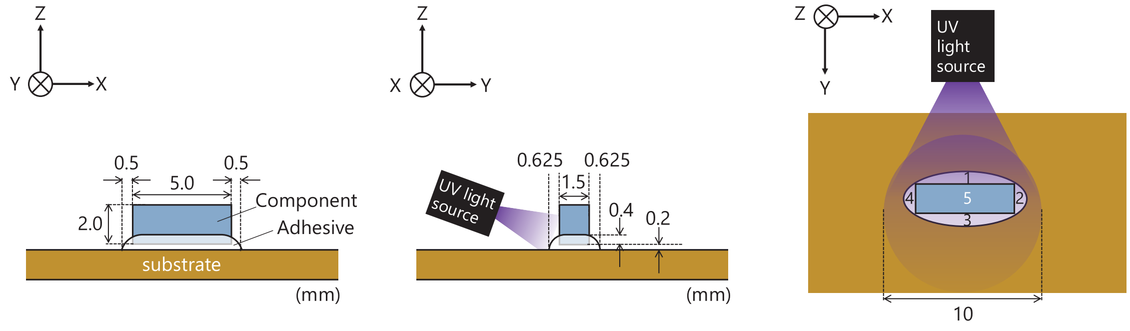

Fig.1. Schematic view of the adhesive structure for simulations and experiments.

light was irradiated for 500 s. The UV irradiance of each area is shown in Table 1. As mentioned above, in cationic polymerization UV curable adhesives, curing continues due to dark reactions even after UV irradiation, so analyses and experiments were conducted even after UV irradiation was stopped. The samples were maintained at 23 °C during and after UV irradiation.

Table 1 UV irradiance in each area of the adhesive.

Area	UV irradiance (mW/cm2)
Area 1	132
Area 2	64
Area 3	49
Area 4	61
Area 5 (bottom of the component)	53

2.2 Formulation of adhesive conversion

To analyze the deformation of the adhesive during the curing process, first, the conversion of the adhesive was measured and formulated [3]. Methods for quantifying the polymerization reaction state of resins include evaluating changes in chemical structure using FT-IR (Fourier transform infrared spectroscopy) and evaluating reaction heat using DSC (differential scanning calorimetry). In this study, a fluorescence-based method was adopted to continuously measure the curing process of the adhesive. The aromatic rings with π electrons contained in epoxy resins would approach each other to form π–π stacking, which releases the energy of the absorbed excitation light as fluorescence. Before curing, π–π stacking is difficult to create owing to the thermal motion in the liquidus state of adhesives, and fluorescence is very weak. However, as the curing reaction progresses, the aromatic rings are stacked as part of the polymer, and the fluorescence from π–πstacking becomes stronger. Based on the above phenomenon, the conversion can be evaluated by changes in fluorescence intensity. In this study, the fluorescence intensities under the same conditions were measured before and after curing, and the normalized difference was defined as the conversion of the adhesive.

The conversion measurement data was fitted to the curing reaction model equations, and the parameters were derived. The reaction must contain an initial curing reaction associated with UV irradiation (p_{uv}) and a dark reaction after UV irradiation (p_{d}). The nth order model [4] [5] was applied to each stage, and their superposition was used as the overall reaction system [6]. They can be expressed as

$$\frac{dp_{\mathrm{uv}}}{dt} = K_{\mathrm{uv}}(1 - p_{\mathrm{uv}}) \tag{1}$$

$$K_{\mathrm{uv}} = k_{\mathrm{uv}} \exp\left(\frac{-c_{\mathrm{uv}}}{RT}\right) = k_{\mathrm{uvT}} \cdot I_{\mathrm{t}}{}^{M} \exp\left(\frac{-c_{\mathrm{uv}}}{RT}\right) \tag{2}$$

$$\frac{dp_{\mathrm{d}}}{dt} = K_{\mathrm{d}}(1 - p_{\mathrm{d}}) \tag{3}$$

$$K_{\mathrm{d}} = k_{\mathrm{d}} \exp\left(\frac{-c_{\mathrm{uv}}}{RT}\right) = k_{\mathrm{dT}} \cdot I_{\mathrm{t}}{}^{N} \exp\left(\frac{-c_{\mathrm{uv}}}{RT}\right) \tag{4}$$

Here, I_{t} is the integrated UV light intensity, t is the time, and T is the temperature. k_{uvT}, M, c_{uv}, k_{dT} and N are experimentally determined constants. The relationship between the rate constants (K_{uv}, K_{d}) and integrated UV light intensity is expressed by a power expression [7], as shown in Equation (2) and Equation (4). Conversions p_{uv} and p_{d} are shown in Fig. 2 (a) and (b), respectively.

2.3 Formulation of adhesive viscoelasticity and deformation

Next, the changes in the viscoelasticity, cure shrinkage, and thermal expansion during curing were measured. These measurements were plotted as a function of the conversion that is described in Section 2.2 and formulated [3]. This makes it possible to calculate physical properties of the adhesive if curing conditions are known.

The viscoelastic properties of the adhesive were measured using a rheometer with a UV irradiation function, operated in oscillatory mode. The relationship between the conversion and moduli is shown in Fig. 3. The elastic modulus during the curing process was formulated into three stages. When the conversion is 0.04 or less, in which gelation was yet to occur. The elastic modulus increases rapidly during this stage. When the conversion is in the range of 0.04 – 0.15, the increase in the elastic modulus slowed down. When the conversion is greater than 0.15, the elastic modulus was almost saturated. The elastic modulus G for the conversion p was fitted using Equations (5), (6), and (7).

$$G = A_1 \cdot \exp(B_1 \cdot p) \qquad (p \leq 0.04) \tag{5}$$

$$G = A_2 \cdot \exp(B_2 \cdot p) \qquad (0.04 \leq p \leq 0.15) \tag{6}$$

$$G = A_3\left(1 - \exp(-B_3 \cdot p)\right) \qquad (p \geq 0.15) \tag{7}$$

Here, A_1,B_1,A_2,B_2,A_3, and B_3 are constants to be determined experimentally.

Furthermore, the mechanical properties of the adhesive change over time because it is viscoelastic material.

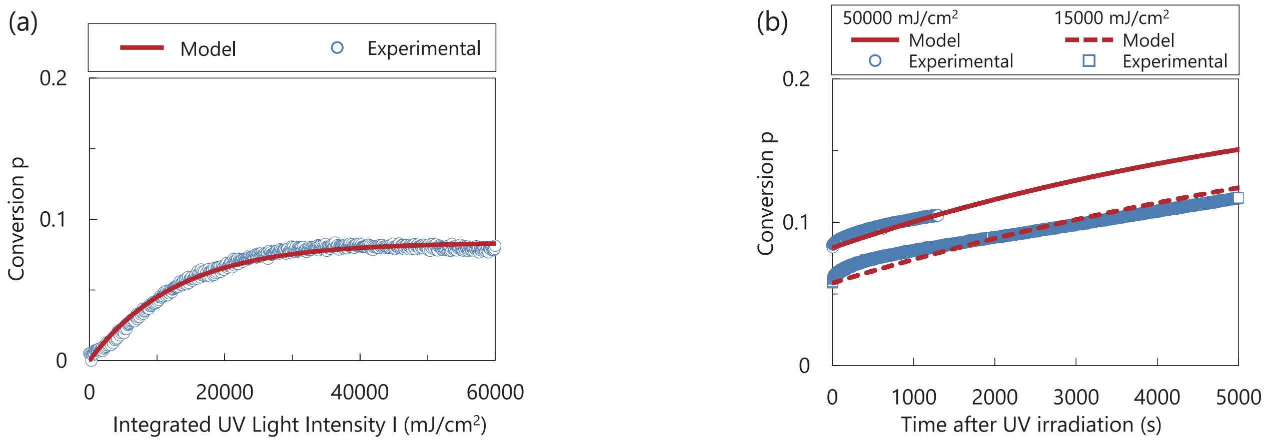

Fig.2. Conversion of the adhesive [9].
(a) Conversion during UV irradiation.
(b) Conversion after UV irradiation.

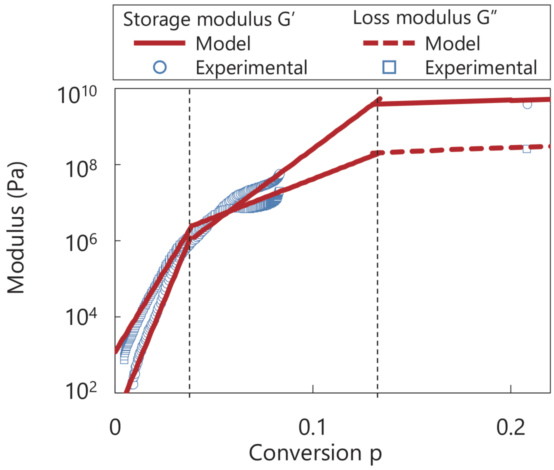

Fig.3. Relationship between the moduli and the conversion 9).

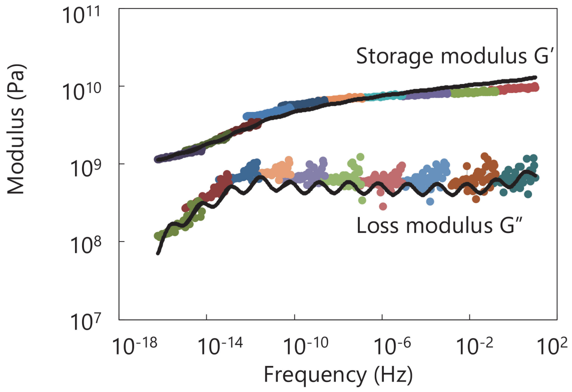

Fig.4. Master curves for storage modulus and loss modulus 9).

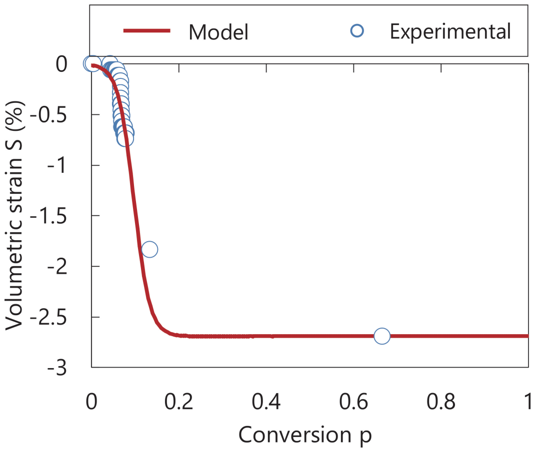

Fig.5. Relationship between the volumetric strain and the conversion 9).

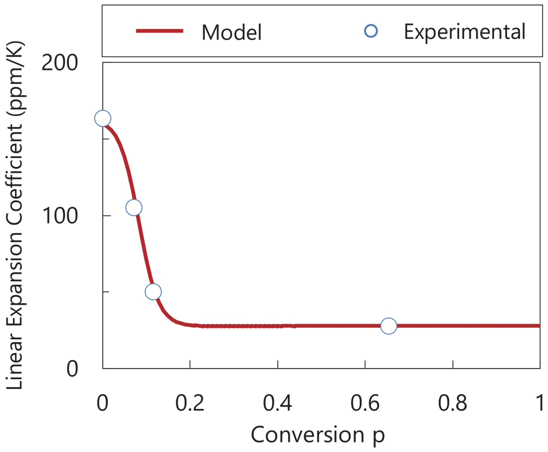

Fig.6. Relationship between the linear expansion coefficient and the conversion 9).

Therefore, the long-term relaxation modulus of the adhesive was formulated using the generalized Maxwell model with the Prony series shown Equation (8). The frequency characteristics of the viscoelasticity of fully cured adhesive samples were measured using DMA (frequency dispersion mode) at temperatures between 25°C and 200°C. Using the time-temperature superposition law, the elastic modulus measurement results obtained at each temperature were shifted horizontally to create master curves shown in Fig. 4. The relaxation function τ_i (T) can be obtained using Equation (9), and the amount of horizontal shift (shift factor a_H (T)) can be obtained using Equation (10) 8).

$$G(t,T) = G_\infty + \sum_{i=1}^{N} G_i \exp\left(\frac{-t}{\tau_i(T)}\right) \qquad (8)$$

$$\tau_i(T) = \frac{1}{\beta_i \cdot a_H(T)} \qquad (9)$$

$$\log a_H(T) = -\frac{A(T-T_{ref})}{B+(T-T_{ref})} \qquad (10)$$

Here, t is the time, T_{ref} is the reference temperature, and A and B are constants to be determined experimentally.

While Fig. 4 shows the relaxation modulus of fully cured adhesive, the change of relaxation modulus of adhesive during the curing was determined using the ratio of the elastic modulus corresponding to the conversion.

The curing shrinkage and the linear expansion coefficient were measured using a laser displacement meter. The sample was the adhesive filled in a metal ring on a glass plate. A UV light source and a temperature-controlled heater were equipped under the glass plate. The curing shrinkage was evaluated by measuring the height of the adhesive surface with the laser displacement meter while the adhesive sample was irradiated with UV light. The linear expansion coefficient was evaluated by measuring the height of the adhesive surface while changing the temperature with the heater. While the thermally induced change in the height is generally proportional to the change in the volume of material, the influence of constrain of the adhesive at the interfaces with the metal ring and the glass plate was corrected. The relationship between the conversion and the curing shrinkage is plotted in Fig. 5, and the relationship between the conversion and the linear expansion coefficient is shown in Fig. 6. The curing shrinkage and the linear expansion coefficient were

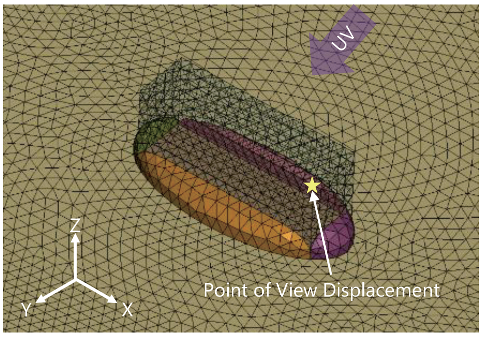

Fig.7. FE model of the adhesive structure.

formulated by fitting with the sigmoid curve shown in equations (11) and (12).

$$S = S_1 \frac{1}{1+\exp(-B_S \cdot (p-p_0))} \tag{11}$$

$$\alpha = (\alpha_0 - \alpha_1) \frac{1}{1+\exp(-b_\alpha \cdot (p-p_0))} + \alpha_1 \tag{12}$$

In Equation (11), S_1 is the shrinkage of the fully cured adhesive and B_S and p_0 are constants determined experimentally. In Equation (12), α_0 and α_1 are the linear expansion coefficients of the uncured and fully cured adhesive respectively, and B_α and p_0 are constants to be determined experimentally.

3. Analyzing displacement of optical components during adhesive curing

3.1 FEM simulation

The implicit solver of the LS-DYNA finite element simulator was used for analysis [9]. The FE model is shown in Fig. 7. All parts were divided into tetrahedral solid elements with a size of 0.3 mm. For the boundary conditions, adhesive/copper substrate and adhesive/glass component interfaces were modeled with shared nodes, and the bottom surface of the copper substrate was fixed in the Z direction.

The glass component and the copper substrate were treated as elastic bodies, and the adhesive part was modeled using *MAT_ADHESIVE_CURING_VISCOELASTIC (MAT_277), a material model in LS-DYNA that can represent the curing of adhesives. Since MAT_277 is a model for heat curable adhesives but not for UV curing, I calculated the conversion caused through UV irradiance by defining it with the curing parameters and temperature of the adhesive. The adhesive part was analyzed on dividing into bodies corresponding to the areas 1–5 as in Fig. 1, each of which was assigned individual parameters corresponding to UV irradiance. Elastic moduli, curing shrinkage, and linear expansion coefficient at each conversion were input to LS-DYNA as curves based on the model in Section 2.3.

3.2 Experimental in situ measurement of displacement

To verify the validity of the analytical method, an experiment was conducted to measure the displacement of the glass component in the adhesive structure shown in Fig. 1 during the curing of the adhesive [9]. A coherence scanning interferometer was used in this experiment, because the measurement must be non-contact to prevent influencing the curing process. As shown in Fig. 8, around a corner of the top surface of the glass component was continuously photographed using the coherence-scanning interferometer, and the displacement of the glass component in the X, Y, and Z directions was derived from the obtained images. The position in the Z direction was calculated from the peak position of the interference fringe intensity, and those in the X and Y directions were calculated from the movement of the contour position by analyzing the images.

3.3 Results and Discussion

The analytical and experimental results of the displacement of the glass component in the X, Y, and Z directions are shown in Fig. 9 (a) to (c). The two results showed similar trends, indicating that the proposed

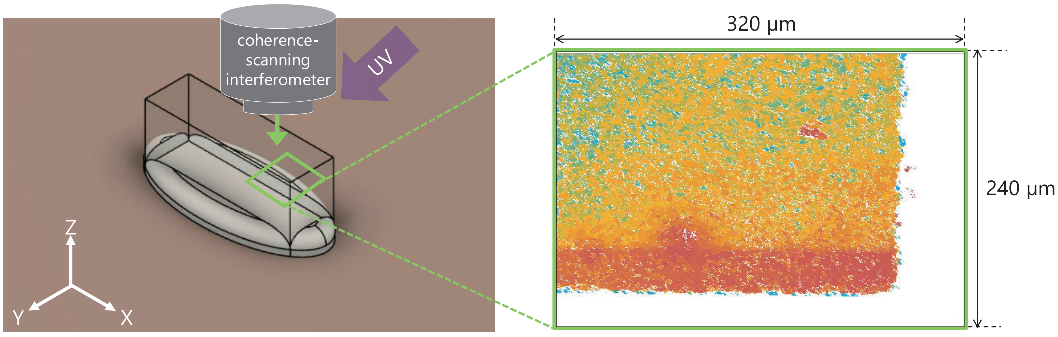

Fig.8. Measuring method for displacements of the optical component.

methodology is effective in predicting curing displacement of optical components. This method is expected to enable efficient design of optical components bonded with a specific adhesive, considering the complexities associated with the curing process.

However, there is a discrepancy between the absolute values of the analysis and the experiment, especially in the Z direction. One of the possible reasons for the gap between the analysis and the experiment is insufficient accuracy in the modeling of the conversion.

Especially, the conversion during the dark reaction process requires careful treatment because physical properties change rapidly. This topic remains a future challenge for the author. Another possible reason is the difference in UV irradiation conditions between the analysis and the experiments. In the analysis, UV irradiation intensity was assumed to be constant in each of Areas 1 to 5 as in Fig. 1. However, the intensity is actually distributed because of absorption by the glass component and the adhesive itself. For a more precise analysis, those absorbances should be taken into account. This topic is also a future challenge for the author.

A notable point in the analytical and experimental results is that most of the displacement of the glass component occurred gradually during the dark reaction process, not during UV irradiation. This suggests that the position and angle of optical components may change over time after UV irradiation, which is an important aspect to consider in the design of manufacturing processes.

Another remarkable point is that the glass component is displaced not only in the Z direction, which is the direction of the thickness of the adhesive layer, but also in the Y direction, which is within the adhesive plane. This phenomenon was probably caused by non-uniform UV irradiation between the adhesive fillets formed on the edges of the two long sides of the glass component. The UV irradiance on one side (Area 1) was 132 mW/cm^2, whereas on the other side (Area 3) it was 49 mW/cm^2, meaning that the irradiance on Area 1 is approximately 2.7 times higher than that of Area 3. In Area 1, which is irradiated with intense UV light, the curing reaction proceeds faster and the curing shrinkage and increase in the elastic modulus occur at a faster rate, causing glass component displacement. While the measured displacement in the X direction after approximately 4 500 s of UV irradiation was 0.4 μm, that in the Y direction was approximately 2.4 μm, which is approximately six times larger. This result suggests that uniform UV irradiation across the entire bonding area is necessary to achieve high positional accuracy.

4. Conclusion

A method was developed to analyze the displacement of optical components bonded with a cationic polymerized UV curable epoxy adhesive. Based on the adhesive curing reaction model, the conversion of the adhesive was formulated. Furthermore, the viscoelasticity and deformation of the adhesive were formulated with respect to the conversion. These equations, describing the adhesive properties, were implemented in FEM simulator to analyze the position of the optical component. To verify the validity of material property modeling and analysis methods, experiments to quantify displacement on adhesively bonded components were also conducted under identical conditions as the simulation.

The analytical and experimental results showed similar trends, indicating that the methodology in this study is effective in predicting curing displacement of optical components. The application of this method can enable efficient development and design of optical products. In both the analysis and the experiment, it was observed that the glass component displacement primarily occurred during the dark reaction process rather than during UV irradiation. Furthermore, in case of non-uniform UV intensity within the irradiation area, the glass component is displaced not only in the direction of adhesive thickness but also in the direction within the adhesive surface.

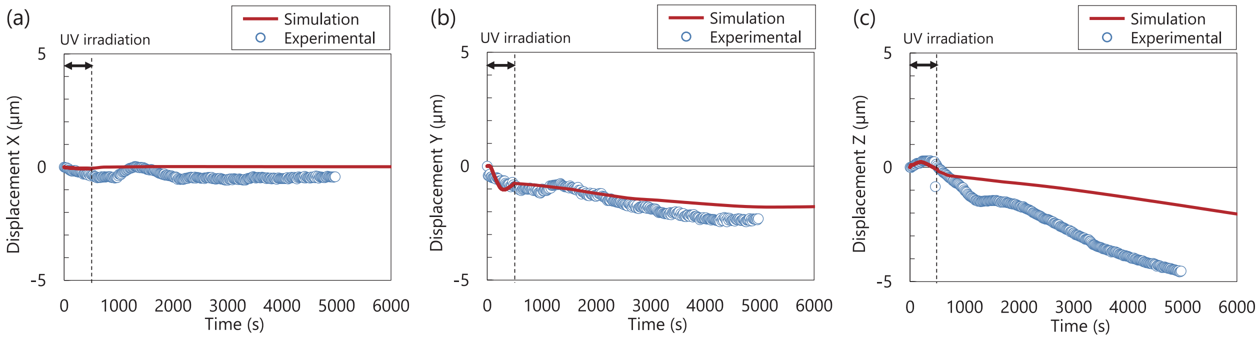

Fig.9. Experimental and Simulation Results for displacements of the optical component [9].
(a) X direction displacement.
(b) Y direction displacement.
(c) Z direction displacement.

ACKNOWLEDGEMENTS

This study was conducted while the author was enrolled in the doctoral program at Tokyo Institute of Technology (now Institute of Science Tokyo). The author expresses sincere appreciation to Professor Chiaki Sato and Associate Professor Yu Sekiguchi (Institute of Science Tokyo, Laboratory for Future Interdisciplinary Research of Science and Technology) for their guidance. The author also thanks Dr. Masahiro Okamura and Mr. Nobuhiro Taki (JSOL Corporation) for their valuable advice regarding the FEM simulator LS-DYNA.

References

1) C. E. Corcione, et al.: “Time–temperature and time-irradiation intensity superposition for photopolymerization of an epoxy based resin” Polymer, Vol.46, pp.8018-8027, 2005.
2) C. Decker, K. Moussa: “Kinetic study of the cationic photopolymerization of epoxy monomers” J. Polym. Sci.: Part A: Polym. Chem., Vol.28, pp.3429–3443, 1990.
3) A. Takahashi, et al.: “Volume change and viscoelastic properties of UV-curable adhesives for precise positioning during curing process and their formulation” J. Adhesion, Vol.98, pp.2029-2044, 2022.
4) G. C. Martin, et al.: “Modeling the structure-property-processing relationships of epoxy resins during cure,” 47th Annual Technical Conference of Society of Plastics Engineers, New York USA, 1989.
5) M. E. Ryan, “Rheological and heat-transfer considerations for the processing of reactive systems,” Polym. Eng. Sci., Vol.24, pp.698-706, 1984.
6) P. L. Chiou, A. Letton: “Modelling the chemorheology of an epoxy resin system exhibiting complex curing behavior” Polymer, Vol.33, pp.3925-3931, 1992.
7) B. Golaz, et al.: “UV intensity, temperature and dark-curing effects in cationic photo-polymerization of a cycloaliphatic epoxy resin” Polymer, Vol.53, pp.2038-2048, 2012.
8) M. L. Williams, et al.: “The temperature dependence of relaxation mechanisms in amorphous polymers and other glass-forming liquids” J. Am. Chem. Soc., Vol.77, pp.3701-3707, 1955.
9) A. Takahashi, et al.: “Analyzing deformation of a cationic photopolymerized epoxy adhesive during the curing process in UV irradiation and dark reaction based on finite element method and measurement” J. Adhesion, Vol.100, pp. 599-615, 2024.